Conformational Stability of Tetrafluorohydrazine, N_2F_4

J. R. Durig* and Zhongnan Shen†

Department of Chemistry, University of Missouri−Kansas City, Kansas City, Missouri 64110-2499

Received: January 7, 1997; In Final Form: May 6, 1997[⊗]

The far infrared (60−350 cm^{-1}) and low-frequency Raman (80−150 cm^{-1}) spectra of gaseous tetrafluorohydrazine, N_2F_4, have been recorded. The fundamental and several excited state transitions of the torsional mode of the *gauche* conformer have been observed in both spectra. Variable-temperature (−60 to −90 °C) studies of the infrared spectra of N_2F_4 dissolved in liquid xenon have been recorded. From these data the enthalpy difference has been determined to be 69 ± 6 cm^{-1} (197 ± 17 cal/mol), with the *trans* conformer the more stable rotamer. *Ab initio* calculations have been carried out with several different basis sets up to MP2/6-311++G* from which the structural parameters, conformational stability, harmonic force constants, and infrared and Raman spectra have been obtained. These quantities have been compared to the experimental values when appropriate. Some of the fundamentals have been reassigned, and the potential function governing the conformer interchange has been determined. The results are compared to the corresponding results from some similar molecules.

Introduction

The structure and conformational stability of tetrafluorohydrazine, N_2F_4, has been extensively investigated by a variety of techniques with considerable controversy.[1−13] From the initial structural study[4] of this molecule, it was concluded that the molecule consists essentially only of the *gauche* conformer in the gas phase at ambient temperature. However, this conclusion was contradicted by analysis of a large amount of vibrational data,[5,6,9,10] along with a reinvestigation of the electron diffraction data[8] which indicated that both the *gauche* and *trans* conformers were present in nearly equal amounts. From a later investigation of the electron diffraction data[11] it was concluded that the *trans* conformer had a higher abundance (70%) than the *gauche* form. Two additional vibrational studies[12,13] have appeared, and the data were interpreted on the basis of a nearly equal *trans*−*gauche* mixture. The initial theoretical calculation[7] gave a conformational stability order of *gauche* > *cis* > *trans*. Clearly from the previous experimental and theoretical findings, there is no doubt about the existence of *gauche* and *trans* rotamers of N_2F_4, but the conformational stability has not yet been determined. Additionally, many different vibrational assignments have been proposed and several interpretations are contradictory.[12] Additionally, the potential function governing the conformational interchange in N_2F_4 has not been determined. Therefore, we have recorded the low-frequency Raman and infrared spectra and carried out extensive *ab initio* calculations.

In the present study, special interest was placed on the conformational stability of N_2F_4. Variable-temperature studies of the infrared spectrum of the sample dissolved in liquid xenon were carried out to determine the enthalpy difference between the stable conformers of N_2F_4. In addition, to provide the theoretical background for a more definitive interpretation of the vibrational spectra, *ab initio* calculations utilizing larger basis sets with electron correlation and normal coordinate analysis were performed. These calculations included the determinations of structural parameters, force constants, frequencies, barriers to internal rotation, and conformational energy difference. The results of these experimental and theoretical results for N_2F_4 are reported herein.

Experimental Section

The sample of N_2F_4 was obtained from the Red Stone Arsenal (Huntsville, AL) and purified on a low-temperature, low-pressure fractionation column. The mid-infrared spectrum of the sample dissolved in liquified xenon was recorded on a Bruker Model IFS 66 Fourier transform interferometer equipped with a Globar source, a Ge/KBr beamsplitter, and a DTGS detector. In this study, the spectra were recorded as a function of temperature ranging from −60 to −90 °C with 100 scans at a resolution of 1.0 cm^{-1} at each temperature. The temperature studies in the liquified noble gas were carried out in a specially designed cryostat cell, which is composed of a copper cell with a 4 cm path length and wedged silicon windows sealed to the cell with indium gaskets. The temperature is monitored by two Pt thermoresistors, and the cell is cooled by boiling liquid nitrogen. The complete cell is connected to a pressure manifold to allow for the filling and evacuation of the cell. After the cell is cooled to the desired temperature, a small amount of sample is condensed into the cell. Next, the pressure manifold and the cell are pressurized with xenon, which immediately starts condensing in the cell, allowing the compound to dissolve.

The Raman spectra were recorded with a Cary Model 82 spectrophotometer equipped with a Spectra-Physics Model 171 argon ion laser tuned to the 5145 Å line. The spectrum of the vapor was recorded using the standard Cary multipass accessory and laser power at the sample of 2 W. The spectrum of the liquid was recorded from a sample sealed under vacuum in a Pyrex glass capillary. The reported frequencies are expected to be accurate to ±2 cm^{-1}.

The far infrared spectrum of the gas, from which the torsional transitions were measured, was recorded with the sample contained in a 1 m cell at a resolution of 0.25 cm^{-1} on a Digilab Model 15B interferometer equipped with a TGS detector and polyethylene windows. Interferograms for both the sample and empty reference cell were recorded 256 times, averaged, and transformed with a boxcar truncation function. Traces of water in the pure sample were removed by passing the gaseous sample

* Author to whom correspondence should be addressed.

† Taken in part from the dissertation of Zhongnan Shen, which was submitted to the Department of Chemistry in partial fulfillment of the Ph.D. degree, May 1996.

⊗ Abstract published in *Advance ACS Abstracts,* June 15, 1997.

S1089-5647(97)00099-0 CCC: $14.00

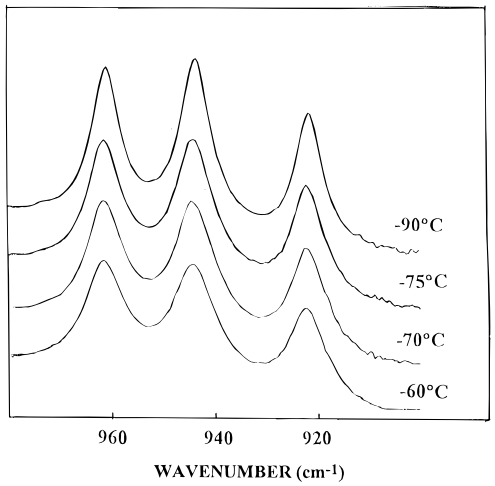

Figure 1. Temperature dependence of the mid-infrared spectra from 900 to 980 cm^{-1} of N_2F_4 dissolved in liquid xenon.

through activated 3 Å molecular sieves using standard high-vacuum techniques.

Conformational Stability

The enthalpy difference between the more stable and high-energy forms of N_2F_4 was obtained from a variable-temperature study of the infrared spectrum of the sample dissolved in liquified xenon. The spectra were recorded at different temperatures varying from −60 to −90 °C. With the advantage of the low temperature and the inertness of the solvent, only small interactions are expected to occur between the dissolved N_2F_4 molecules and the noble gas atoms. The recorded conformer peaks are well resolved compared with the ones observed in the mid-infrared spectrum of the gas.

The mid-infrared absorption spectra in the region 970−900 cm^{-1} of N_2F_4 dissolved in xenon are shown in Figure 1. The two bands centered at 944 (*trans*) and 962 (*gauche*) cm^{-1} were selected for the ΔH determination. Upon decreasing the temperature of the solution, the relative intensity of the 944 cm^{-1} band (*trans*) slightly increases relative to the 962 cm^{-1} band. This indicates that the *trans* conformer is the more stable species. The intensities of this conformational doublet were fit to the equation

$$-\ln(I_{trans}/I_{gauche}) = \Delta H/RT - \ln(\epsilon_{trans}/\epsilon_{gauche}) - \Delta S/R$$

where ϵ is the absorption coefficient and it is assumed that ϵ, ΔH, and ΔS are not a function of the temperature in the experimental temperature range. A van't Hoff plot was constructed (Figure 2) from the data, and the value of the enthalpy difference, ΔH, was determined experimentally to be 69 ± 6 cm^{-1} (197 ± 17 cal/mol). This enthalpy value from the rare gas solution should be close to the value in the vapor[14] since the volumes of the two conformer molecules and their dipole moments do not differ significantly.

Additionally, the ΔH value was determined utilizing the predicted Raman activities from the *ab initio* calculations along with the relative intensities (peak height) of five Raman lines for each conformer (Figure 3) in the region below 700 cm^{-1}. The product of the Raman activity times the peak height was utilized for the intensity term in the van't Hoff equation for each Raman line. By this method a value of ΔH in the liquid phase was calculated to be 25 ± 4 cm^{-1} (88 ± 14 cal/mol), and again the data indicate that the *trans* form is the thermodynamically preferred conformer.

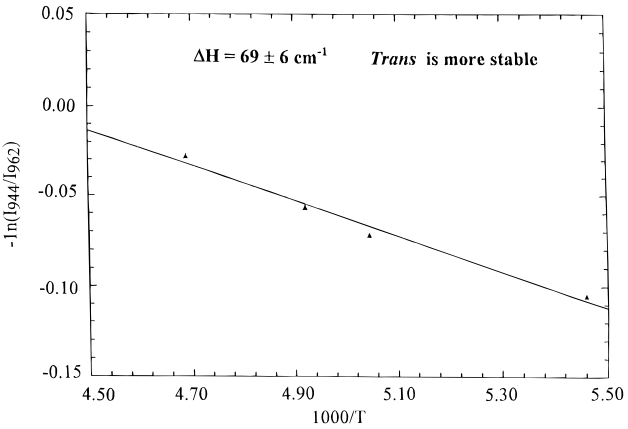

Figure 2. van't Hoff plot for N_2F_4 dissolved in liquid xenon.

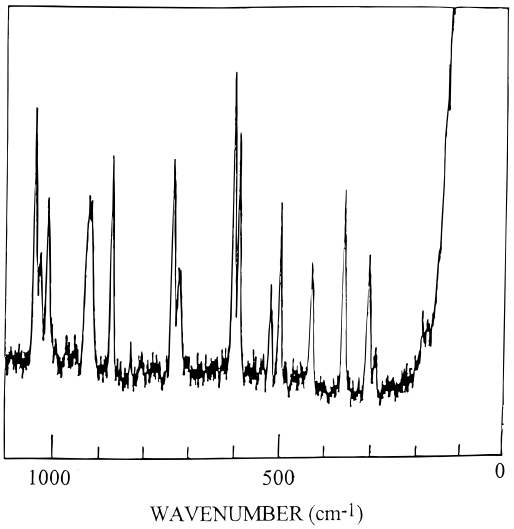

Figure 3. Raman spectrum of glassy N_2F_4.

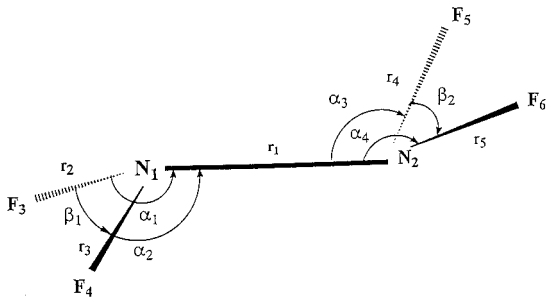

Figure 4. Atom numbering and internal coordinates for the *trans* conformer of N_2F_4.

Ab Initio Calculations

The *ab initio* calculations were carried out using the Gaussian-92 program.[15] Complete geometry optimizations have been performed by means of the analytical gradient method of Pulay.[16] The calculated structural parameters, rotational constants, dipole moments, and energies for both *trans* and *gauche* conformers using various basis sets are listed in Table 1. The force constants have been obtained from analytical second derivatives of the electronic energy with respect to the nuclear coordinates for each optimized geometry. The force constants calculated have been used to determine the harmonic vibrational frequencies. The frequencies predicted at the MP2/6-311++G* level of theory were calculated numerically due to computer limitations.

The atom numbering of N_2F_4 is shown in Figure 4. An examination of the optimized structural parameters listed in

TABLE 1: Comparison of Computed and Experimental Structural Parameters[a] and Energies for Tetraflurohydrazine (N_2F_4) Conformers

	MP2/6-31G*		RHF/6-311++G**		MP2/6-311++G**		microwave[b]	ED[c]		ED[d]
parameter	*gauche*	*trans*	*gauche*	*trans*	*gauche*	*trans*	*gauche*	*gauche*	*trans*	*gauche/trans*
r(N−N)	1.463	1.499	1.4032	1.438	1.456	1.503	1.47	1.489 ± 0.004	1.489 ± 0.004	1.492 ± 0.007
r(N−F_3)	1.392	1.390	1.3284	1.324	1.377	1.371	1.37	1.375 ± 0.004	1.375 ± 0.004	1.372 ± 0.002
r(N−F_4)	1.389	1.390	1.3234	1.324	1.370	1.371	1.37	1.375 ± 0.004	1.375 ± 0.004	1.372 ± 0.002
∠NNF_3	105.9	99.2	108.69	102.3	107.7	100.3	104 ± 3	104.3 ± 1.0	102.9 ± 1.0	101.4 ± 0.4
∠NNF_4	100.1	99.2	103.52	102.3	101.4	100.3	104 ± 3	100.1 ± 1.5	100.0 ± 0.8	101.4 ± 0.4
∠FNF	102.7	102.7	103.80	103.7	103.3	103.3	108 ± 3	105.1 ± 1.5	102.9 ± 1.0	103.1 ± 0.6
dihedral angle, φ	63.9	180.0	68.94	180.0	67.1	180.0	65 ± 3	67.1 ± 1.0	180.0	64.2 ± 3.7
$\lvert\mu_a\rvert$	0.000	0.0	0.000	0.0	0.000	0.0				
$\lvert\mu_b\rvert$	0.000	0.0	0.000	0.0	0.000	0.0				
$\lvert\mu_c\rvert$	0.521	0.0	0.377	0.0	0.601	0.0				
$\lvert\mu_t\rvert$	0.521	0.0	0.377	0.0	0.601	0.0	0.26			
A	5527.3	5272.5	5981.4	5786.1	5578.5	5392.5	5576.21			
B	3280.4	3585.8	3305.8	3735.1	3202.7	3563.0	3189.35			
C	2842.4	2253.5	2952.2	2375.9	2819.4	2258.1	2812.95			
−(E + 506), au	1.343 319	1.342 330	0.458 064	0.455 5401	1.748 271	1.747 677				
ΔE, cm^{-1}		217		554		130				

[a] Bond distances in angstroms, bond angles in degree, dipole moments in debye, and rotational constants in MHz. [b] Reference 1. [c] Reference 8. [d] Reference 11, where the parameters were assumed to be the same for both conformers except for the dihedral angle.

Table 1 shows that the most interesting structural feature is the geometry modifications on going from the *trans* to the *gauche* conformer. These involve the changes of the N−N bond length and the bond angles ∠NNF_3 and ∠NNF_4. The predicted N−N bond length for the *gauche* conformer is much shorter than that for the *trans* form by 0.03−0.05 Å irrespective of the basis sets. In contrast, one of the N−F bond distances lengthens about 0.006 Å, whereas the other N−F bond parameter remains almost the same in going from the *trans* to the *gauche* conformer. In addition, the bond angles calculated with all basis sets show the same trend with the ∠NNF_3 bond angle opening by ∼6−8° when the conformation changes from the *trans* form to the *gauche* conformer, whereas the ∠NNF_4 angle opens by only ∼1° during the same conformation change. This large ∠NNF_3 angle in the *gauche* form is attributed to the strong interaction between the two adjacent N−F polar bonds in the *gauche* conformer compared to the *trans* configuration. However, it should be noted that the FNF bond angle remains the same during the conformational interchange. The calculated dihedral angle at the MP2 level with the largest basis set is within the experimental error of the value reported from the electron diffraction studies.[8,11]

The rotational constants obtained from the MP2/6-311++G* calculation are in reasonable agreement with the values from the microwave study, but the dipole moment is about twice the reported value.[1] However, the authors[1] indicated that the value of 0.26 D was only a preliminary value and no uncertainty in the value was indicated. A more definitive measurement of the value of the dipole moment would be valuable for comparison to the theoretical value. Also, since the calculated B rotational constant differs by 13 MHz from the experimental value, we attempted to fit the rotational constants by varying the angles.

A normal coordinate analysis was carried out in order to obtain more information on the molecular motions involved in the fundamental vibrations of N_2F_4. This analysis was performed utilizing *ab initio* calculations and the Wilson FG matrix method[17] with the normal coordinate program originally written by Schachtschneider.[18] The internal coordinates are shown in Figure 4. This complete set of internal coordinates was used to construct 12 symmetry coordinates. The **B** matrix was used to convert the *ab initio* force field in Cartesian coordinates to a force field in internal coordinates using a program developed in our laboratory. These values are available upon request. For frequencies calculated at the MP2/6-31G* level, a set of scaling factors of 0.9 for both stretching and bending and 1.0 for the torsion was used to obtain the fixed scaled frequencies and potential energy distribution (PED) expressed in terms of the symmetry coordinates. No scaling procedure was used for frequencies calculated at the MP2/6-311++G* level.

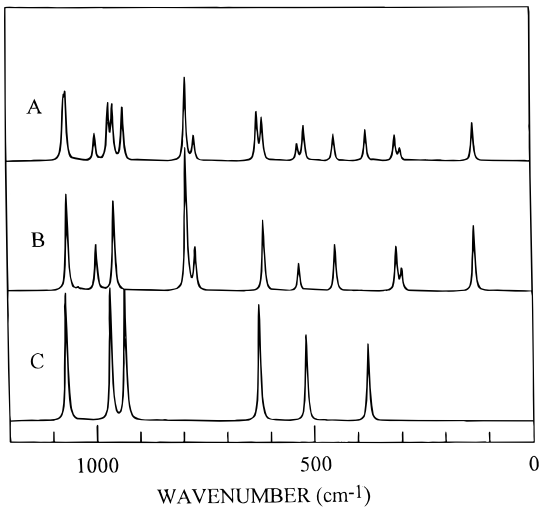

Figure 5. Simulated Raman spectra of N_2F_4: (A) mixture of *trans*−*gauche* conformers; (B) pure *gauche* form; (C) pure *trans* form.

The Raman spectrum for N_2F_4 was calculated using the results from the *ab initio* calculations. The Raman scattering cross sections, $\partial\sigma_j/\partial\Omega$, which are proportional to the Raman intensities, can be calculated as described previously.[19,20] Utilizing these Raman scattering cross sections, frequencies, intensities, and depolarization ratios have been calculated. Taking these data and a Lorentzian line-shape function, the theoretical Raman spectrum was calculated (Figure 5). The predicted spectrum should be compared to the experimental one shown in Figure 3.

Vibrational Assignment

In spite of several studies of the vibrational spectra of N_2F_4 that have been published,[5,6,9,10,12,13] there are still a few questions on the assignments of the fundamentals. The previous assignments have been based on the following considerations: comparison of the infrared and Raman spectra, the depolarization ratios of the fundamental Raman bands, band contours in the

infrared spectrum of the gas, and symmetry considerations. Since there have been no previous normal coordinate calculations for this molecule, we have carried out such a study utilizing the *ab initio* force constants to support the vibrational assignment.

In general, there is good agreement between the simulated (Figure 5) and the experimental (Figure 3) Raman spectra, particularly in the region below 800 cm^{-1}. The bands centered at 733 and 719 cm^{-1} were previously assigned[12] to the NF_2 wagging modes in the *gauche* and *trans* conformers, respectively. However, as can be seen from the calculated spectrum, both of these bands belong to the *gauche* conformer. Therefore, the band at 733 cm^{-1} is reassigned to the N−N stretch and the other one at 719 cm^{-1} to the NF_2 wag for the *gauche* conformer.

With the 719 cm^{-1} band no longer being assigned to the *trans* conformer (A_g mode) it is necessary to assign a polarized Raman line without an infrared counterpart to the *trans* conformer. The choices are very limited, with the *ab initio* calculations predicting this fundamental in the range 870−940 cm^{-1}. We have chosen the Raman Q-branch at 931 cm^{-1} in the spectrum of the gas, even though the corresponding line in the liquid appears depolarized. The other possible choice is the 873 cm^{-1} Raman line, but the Raman band of the gas clearly indicates that this band is a B_g mode. The only other change in the assignment of the fundamentals for the *trans* conformer is the infrared band in the spectrum of the gas at 949 cm^{-1} (944 cm^{-1} in the xenon solution) which is assigned as the NF_2 antisymmetric stretch (A_u). This mode had been assigned to the band at 962 cm^{-1}, but it is now assigned to the *gauche* conformer. Also, it is believed that the torsional mode has not been observed in the far infrared spectrum for the *trans* conformer particularly since it is predicted to be 100 times weaker than the NF_2 twist at 252 cm^{-1}.

The assignment of a second fundamental in the 700 cm^{-1} region for the *gauche* conformer requires the deletion of another band previously assigned to this conformer.[9,12,13] The obvious choice is the 242 cm^{-1} infrared band, which is probably the P branch of the ν_6 fundamental (252 cm^{-1}) of the *trans* conformer. There may be some contribution from the overtone of the torsional mode to the 242 cm^{-1} infrared absorption.

The most confusing region of the vibrational spectrum in terms of normal mode assignment is the N−F stretching region (1000−900 cm^{-1}). The Raman line at 922 cm^{-1} in the spectrum of the liquid probably consists of two overlapping bands ∼960 and 931 cm^{-1}, which belong to the *gauche* and *trans* conformers, respectively. The one puzzle remaining is the band at 1010 cm^{-1}, which, according to the Raman spectra of the gas and liquid, is a strong, polarized peak. However, our calculations cannot match this line by both intensity and depolarization ratio. One possibility is to assign this line to the NF_2 antisymmetric stretch (A) for the *gauche* conformer on the basis of the Raman intensity. However, the *ab initio* calculations indicate that this fundamental should be at a much lower frequency, with a depolarization ratio of 0.74. An alternative is to assign the 1012 cm^{-1} Raman line as a Fermi doublet ($2\nu_{11}$) with the 1027 cm^{-1} fundamental (ν_1) and then assign the ν_2 fundamental as essentially degenerate with the ν_8 fundamental of the *trans* conformer. Such an assignment is attractive since it explains the observation of an infrared band at 873 cm^{-1} which cannot be the ν_8 fundamental of the *trans* conformer. This lower frequency for ν_2 for the *gauche* conformer is consistent with the *ab initio* prediction for this fundamental. The assignment of the 1012 and 1027 cm^{-1} Raman lines as a Fermi doublet helps explain why the relative intensity of these two lines changes significantly from their intensities in the gas to those in the liquid.

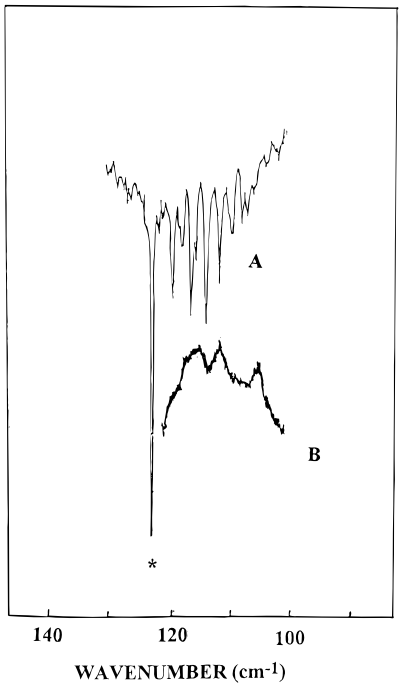

Figure 6. Far infrared spectrum (A) and Raman spectrum (B) of gaseous N_2F_4. Band marked with an asterisk is due to rotational transition of the HF impurity.

For the torsional fundamentals, the symmetry requires the band observed in the Raman spectrum of the gas to belong to the *gauche* form (Figure 6). This line has essentially the same frequency as the torsional mode observed in the infrared spectrum (Figure 6). Since the infrared intensity of the torsional mode for the *trans* form is calculated to be 10 times weaker than the corresponding *gauche* fundamental, it is believed that the torsional mode was not observed for the *trans* conformer. Assuming the same deviations between calculated and observed frequencies (10 cm^{-1}) for both conformers, a value of 107.0 cm^{-1} is estimated for the *trans* torsional (1←0) fundamental. The assignments for the fundamentals for both conformers are summarized in Tables 2 and 3.

Torsional Potential Function

According to the *ab initio* calculations, the energy difference between the *trans* and *gauche* conformers is 130 cm^{-1} (372 cal/mol) at the MP2/6-311++G* level, with the *gauche* rotamer the more stable form. Calculations with smaller basis sets or at the RHF level gave even larger values, all favoring the *gauche* form as the more stable conformer. The potential surface governing the internal rotation was calculated at the MP2/6-311++G* level by allowing the torsional dihedral angle to vary by 30 deg increments with full relaxation of all other structural parameters. The transition state connecting the two conformers was confirmed by one imaginary frequency. The calculated energies were then analyzed in terms of a potential function which is represented as a Fourier cosine series in the internal rotation angle φ:

$$V(\varphi) = {}^1/_2 \sum_{i=1}^{6} V_i(1 - \cos i\varphi)$$

The potential constants V_i and the potential function calculated with the MP2/6-311++G* basis set are given in Table 4 and depicted graphically in Figure 7.

The potential function governing the internal rotation can also be obtained from the observed torsional transitions (Table 5),

TABLE 2: Comparison of Experimental and Computed Infrared and Raman Frequencies of *trans*-Tetrafluorohydrazine

species	vib. no.	description	MP2/6-311++G*** calc	MP2/6-31G* calc	MP2/6-31G* scaled[a]	IR int.[b]	Raman act.[c]	dp ratio	infrared[d] gas	infrared[d] soln	Raman[d] gas	Raman[d] liquid	Raman[d] solid	PED
A_g	ν_1	NF_2 symmetric stretch	1068	1067	1013	0.0	16.8	0.29			1036	1036	1038	$54S_1,19S_3,27S_4$
	ν_2	N−N stretch	933	947	898	0.0	14.4	0.19			931	923	922	$51S_2,14S_1,34S_4$
	ν_3	NF_2 scissor	625	610	579	0.0	7.8	0.16			601	600	602	$47S_3,32S_1,16S_2$
	ν_4	NF_2 wag	376	372	353	0.0	2.6	0.43			354	354	359	$34S_4,33S_2,34S_3$
A_u	ν_5	NF_2 antisymmetric stretch	981	1007	959	225.7	0.0	0.0	947	949				$100S_5$
	ν_6	NF_2 twist	259	252	240	1.5	0.0	0.0	252	(252)				$95S_6$
	ν_7	torsion	117	120	120	0.01	0.0	0.0						$93S_7$
B_g	ν_8	NF_2 antisymmetric stretch	966	978	928	0.0	15.3	0.75			873	867	873	$68S_8,32S_9$
	ν_9	NF_2 twist	517	518	491	0.0	4.5	0.75			494	494	498	$68S_9,32S_8$
B_u	ν_{10}	NF_2 symmetric stretch	1039	1047	993	115.6	0.0	0.0	999	993				$84S_{10},15S_{11}$
	ν_{11}	NF_2 scissor	554	532	505	4.0	0.0	0.0	542	540				$83S_{11}$
	ν_{12}	NF_2 wag	488	479	455	5.7	0.0	0.0	467	468				$94S_{12}$

[a] Scaled *ab initio* calculations with factors of 0.9 for stretching and bending, 1.0 for torsion. [b] Calculated infrared intensities in km mol^{-1} using the MP2/6-31G* basis set. [c] Calculated Raman intensities in $Å^4\ u^{-1}$ using the RHF/6-31G* basis set. [d] Observed frequencies taken from ref 12 with some reassignments.

TABLE 3: Comparison of Experimental and Computed Infrared and Raman Frequencies of *gauche*-Tetrafluorohydrazine

species	vib. no.	description	MP2/6-311++G** calc	MP2/6-31G* calc	MP2/6-31G* scaled[a]	IR int.[b]	Raman act.[c]	dp ratio	infrared[d] gas	infrared[d] liquid	Raman[d] gas	Raman[d] liquid	Raman[d] solid	PED
A	ν_1	NF_2 symmetric stretch	1063	1058	1004	16.2	12.6	0.19	1023	1025	1027	1025	1026	$63S_1,18S_3$
	ν_2	NF_2 antisymmetric stretch	956	981	931	81.6	10.2	0.74	873	1010	873	873		$69S_5,16S_6$
	ν_3	N−N stretch	790	806	764	3.9	12.9	0.04	737	733	733	733	736	$68S_2,17S_4$
	ν_4	NF_2 scissor	613	596	565	2.0	4.6	0.25	590	588	587	590	590	$41S_3,26S_1,15S_6$
	ν_5	NF_2 twist	449	446	422	0.1	2.0	0.67		423	423	430	430	$33S_6,40S_3,15S_2$
	ν_6	NF_2 wag	310	324	308	0.4	1.1	0.53	300	300	298	304	304	$69S_4,26S_6$
	ν_7	torsion	130	144	144	0.1	0.4	0.74	120	122	120			$100S_7$
B	ν_8	NF_2 symmetric stretch	1039	1049	995	102.8	0.3	0.75	958	960	960	960	960	$61S_{10},20S_8,14S_{11}$
	ν_9	NF_2 antisymmetric stretch	997	1015	963	88.8	5.5	0.75	946			922	922	$53S_8,31S_{12},10S_9$
	ν_{10}	NF_2 wag	770	771	731	50.9	3.6	0.75			719	719	723	$47S_{12},26S_8,25S_{10}$
	ν_{11}	NF_2 scissor	532	510	484	2.0	1.5	0.75	518	515		515	515	$77S_{11},11S_{10},11S_{12}$
	ν_{12}	NF_2 twist	298	301	285	1.3	0.5	0.75	284	284	288	288	288	$85S_9,10S_{12}$

[a] Scaled *ab initio* calculations with factors of 0.9 for stretching and bending, 1.0 for torsion. [b] Calculated infrared intensities in km mol^{-1} using the MP2/6-31G* basis set. [c] Calculated Raman intensities in $Å^4\ u^{-1}$ using the RHF/6-31G* basis set. [d] Observed frequencies taken from ref 12 with some reassignments.

TABLE 4: Internal Rotational Barriers and Potential Function for Tetrafluorohydrazine

parameter	MP2/6-311++G**	calculation[a]
V_1	−1445	-1729 ± 62
V_2	−1459	-1367 ± 53
V_3	−2449	-2192 ± 30
V_4	−30	-152 ± 8
V_5	−19	
V_6	109	130 ± 10
gauche to *trans* barrier, cm^{-1}	1857	1487
trans to *gauche* barrier, cm^{-1}	1726	1419
gauche to *gauche* barrier, cm^{-1}	4041	3863
torsional dihedral angle (*gauche)*	67.1	67.1
$\Delta E_{gauche-trans}$, (cm^{-1})	-130	69 ± 6

[a] Calculation is based on the observed far infrared transitions listed in Table 5 along with the ΔH value from the xenon solution and the *gauche* dihedral angle from ref 8.

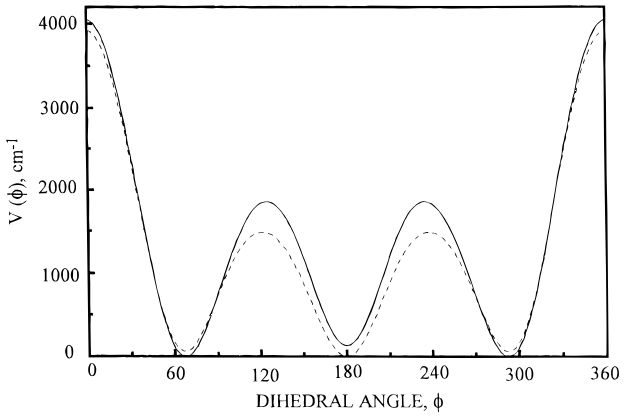

Figure 7. Torsional potential functions of N_2F_4. Solid line is *ab initio* predicted potential and dotted line is experimental potential.

along with the enthalpy difference between the conformers and the dihedral angle of the *gauche* conformer. The torsional dihedral angular dependence of the internal rotation constant, $F(\varphi)$, can be represented as a Fourier series:

$$F(\varphi) = F_0 + \sum_i F_i \cos i\varphi$$

Since the structural parameters are different for the two conformers, the calculation of the kinetic term, or the F series, becomes rather complicated since it is also a function of the dihedral angle φ. The relaxation of the structural parameters during the internal rotation can be incorporated into the above equation by assuming that they are small periodic functions of the torsional angle of the general type

$$B(\varphi) = a + b \cos \varphi + c \sin \varphi$$

The series coefficients were calculated using the optimized structural parameters from the *ab initio* calculations. The experimental torsional potential function was calculated by an iterative weighted nonlinear least-squares fitting of the observed torsional frequencies for the *gauche* rotamer, the estimated frequency for the torsional fundamental of the *trans* form, the ΔH obtained from the xenon solution, and the *gauche* dihedral angle. The potential constants obtained from these data are listed in Table 4, and the potential function is shown in Figure 7.

TABLE 5: Observed and Calculated (cm^{-1}) Asymmetric Torsional Transitions for N_2F_4

transition	obs	calc	Δ
gauche			
1←0	120.0	119.8	0.2
2←1	117.2	117.2	0.0
3←2	114.4	114.5	−0.1
4←3	112.2	112.3	−0.1
5←4	110.2	110.0	0.2
trans			
1←0	107.0 (assumed)	107.3	−0.3

TABLE 6: Observed and Calculated (cm^{-1}) Asymmetric Torsional Transitions for N_2F_4

transition	obs	calc	Δ
gauche			
1←0	120.0	119.8	0.2
2←1	117.2	117.2	0.0
3←2	114.4	114.5	−0.1
4←3	112.2	112.3	−0.1
5←4	110.2	110.0	0.2
trans			
1←0	107.0 (assumed)	107.3	−0.3

Discussion

As can be seen from the data in Table 1, the inclusion of electron correlation by the MP2 method gives a more realistic geometry for the N_2F_4 molecule. Even so, there still exists significant differences between the predicted and experimentally determined distances. On the other hand, the simulated Raman spectrum provides a rather stringent test of the calculation, where the remarkably good agreement with the experimental data supports the conclusion that the force field, relative Raman intensities, and the PED for each conformer are reasonable.

Of particular note is the predicted Raman spectrum relative to the experimental determined spectrum in the region below 800 cm^{-1}, where the relative intensities agree so well. These data clearly show the value of predicting both the frequencies and the intensities of the Raman spectrum for conformational studies of small molecules. They are also very helpful for making the vibrational assignment as well as distinguishing which lines belong to which conformer.

It is clear from the structural parameters obtained from the *ab initio* calculations irrespective of the basis set or the level of calculation that the two conformers have significantly different N−N distances. Therefore, a re-analysis of the electron diffraction data taking the predicted differences in the N−N distance as well as the angles of the inner and outer NF bonds between the two conformers should result in a significant improvement in the knowledge of the structural parameters for N_2F_4. It is believed that the *ab initio* data could be very useful in providing a definitive structure from the previously obtained electron diffraction curves. Such structural information could be very useful in accessing the errors in the predicted parameters from the *ab initio* calculations.

The temperature study of the infrared spectrum gave an enthalpy difference of 69 ± 6 cm^{-1} (197 ± 17 cal/mol) with the *trans* conformer the more stable rotamer. This conclusion is supported by the calculations utilizing the predicted Raman activities along with the relative intensities of the observed lines in the experimental Raman spectrum. Inspection of the previously reported Raman spectra in the solid phase where lowering the temperature resulted in a slight increase of the relative intensity of bands due to the *gauche* form can be explained as due to dipole−dipole interactions, which will stabilize the *gauche* conformer in the solid state. The enthalpy determined from liquified xenon solution can be considered as a "pseudo gas phase" value.[14] Therefore, the experimental spectroscopic data indicate that the *trans* conformer of N_2F_4 is the more stable form of this molecule. With such a small enthalpy difference *ab initio* calculations cannot be expected to predict the more stable rotamer.

It is interesting to compare the potential function of N_2F_4 with those for some analogous molecules. Examining the data in Table 4 shows large values of V_1 and V_3, which indicates a rather large barrier to internal rotation. The contributions from both the large and negative V_2 (indicating that the lone pair orbitals on adjacent N atoms prefer to be orthogonal) and the V_3 terms favor the *gauche* form around 60°. The combination of these contributions results in two stable conformers with almost equal energies. The P_2F_4 molecule is expected to have significant bonding similarities to N_2F_4. It is interesting to note that the calculated V_i terms[21] for P_2F_4 have values of the potential constants of $V_1 = -1842$, $V_2 = -84$, and $V_3 = -503$ cm^{-1}. Although both *gauche* and *trans* conformers can be expected for the P_2F_4 molecule, the small value of the V_2 term leads to a shallow potential well around 70°, which corresponds to the *gauche* conformer. Because of its small barrier, it is reasonable to expect that only the *trans* form will be observed experimentally at ambient temperature for the P_2F_4 molecule.[22]

It was somewhat surprising to find that the N−N stretching frequencies between the *gauche* and *trans* conformer are separated by ∼200 cm^{-1}, whereas their N−N bond distances are predicted as 1.456 Å (*gauche*) and 1.503 Å (*trans*) from the MP2/6-311++G* calculation. The conformer with the shorter bond length has the lower vibrational frequency, a reversal of what one might expect. This disparity shows that the correlations between the vibrational frequencies and the relative bond lengths are not always straightforward, as also found for the case of some boron−phosphorus complexes.[23]

It should be noted that the force constants for the two conformers reflect the differences in the structural parameters for the two rotamers. For example the N−N stretching constant for the *gauche* form with a value of 3.326 mdynes/Å is significantly larger than the value of 2.906 mdynes/Å for this force constant for the *trans* rotamer. Similar differences are also found for the force constants for the N−F strengths and the FNN angle bends. However, for the FNF angle, which is the same for both rotamers, the force constants are nearly the same.

The potential energy distributions obtained from the *ab initio* calculations indicate that the descriptions of several of the fundamental vibrations need to be significantly altered. For example, the band at 601 for the *trans* conformer had previously been fairly uniformly assigned as an N−N stretch, whereas it is made up of 47% NF_2 scissoring motion, 32% NF_2 symmetric stretch, and only 16% N−N stretch. In fact, the band at 931 cm^{-1} has 52% N−N stretch and 34% NF_2 wag. Similarly the band at 587 cm^{-1}, which had been assigned as the N−N stretch for the *gauche* conformer, is made up of 41% NF_2 scissors and 26% NF_2 symmetric stretch with no contribution from the N−N stretching mode. For the *gauche* molecule the band at 733 cm^{-1} is 68% N−N stretch and 17% NF_2 wag. Other major changes in the descriptions of the bands are the NF_2 wag which has a lower frequency than the NF_2 scissors for the B_u modes of the *trans* conformer as well as for the A modes of the *gauche* conformer. However, for the B modes of the *gauche* conformer the order is NF_2 wag, NF_2 scissor, and NF_2 twist, where the latter two are reversed from the assignment previously proposed.[12] However, it should be noted that only the assignments for three fundamental frequencies have been altered from those

given earlier.[12] Nevertheless, the *ab initio* calculations have proven invaluable in the interpretation of the infrared and Raman spectra.

Acknowledgment. J.R.D. would like to acknowledge partial support of these studies by the University of Missouri—Kansas City Faculty Research Grant program.

References and Notes

(1) Lide, D. R., Jr.; Mann, D. E. *J. Chem. Phys*. **1959**, *31*, 1129.
(2) Durig, J. R.; Lord, R. C. *Spectrochim. Acta* **1960**, *16*, 1471.
(3) Colburn, C. B.; Johnson, F. A.; Haney, C. *J. Chem. Phys*. **1965**, *43*, 4526.
(4) Bohn, R. K.; Bauer, S. H. *Inorg. Chem*. **1967**, *6*, 304.
(5) Durig, J. R.; Clark, J. W. *J. Chem. Phys*. **1968**, *48*, 3216.
(6) Koster, D. F.; Miller, F. A. *Spectrochim. Acta* **1968**, *24A*, 1487.
(7) Cowley, A. H.; White. W. D.; Damasco, M. C. *J. Am. Chem. Soc*. **1969**, *91*, 1922.
(8) Cardillo, M. J.; Bauer, S. H. *Inorg. Chem*. **1969**, *8*, 2086.
(9) Oskam, A.; Elst, R.; Dunker, J. C. *Spectrochim. Acta* **1970**, *26A*, 2021.
(10) Selig, H.; Holloway, J. H. *J. Inorg. Nucl. Chem*. **1971**, *33*, 3169.
(11) Gilbert, M. M.; Gundersen, G.; Hedberg, K. *J. Chem. Phys*. **1972**, *56*, 1691.
(12) Durig, J. R.; MacNamee, R. W. *J. Raman Spectrosc*. **1974**, *2*, 635.
(13) Shchepkin, D. N.; Zhygula, L. A.; Belozerskaya, L. P. *J. Mol. Struct*. **1978**, *49*, 265.
(14) Herrebout, W. A.; van der Veken, B. J.; Wang, Aiying; Durig, J. R. *J. Phys. Chem*. **1995**, *99*, 578.
(15) Frisch, M. J.; Trucks, G. W.; Head-Gordon, M.; Gill, P. M. W.; Wong, M. W.; Foresman, J. B.; Johnson, B. G.; Schlegel, H. B.; Robb, M. A.; Replogle, E. S.; Gomperts, R.; Andres, J. L.; Raghavachari, K.; Binkley, J. S.; Gonzalez, C.; Martin, R. L.; Fox, D. J.; Defrees, D. J.; Baker, J.; Steward, J. J. P.; Pople, J. A. *Gaussian 92*; Gaussian, Inc.: Pittsburgh, PA, 1992.
(16) Pulay, P. *Mol. Phys*. **1969**, *17*, 197.
(17) Wilson, E. B.; Decius, J. C.; Cross, P. C. *Molecular Vibration*; McGraw-Hill: New York, 1955.
(18) Schachtshneider, J. H. *Vibrational Analysis of Polyatomic Molecules*; Shell Development Company Report, Emeryville, CA, 1964; Vol. VI.
(19) Durig, J. R.; Davis, J. F.; Guirgis, G. A. *J. Raman Spectrosc*. **1994**, *25*, 189.
(20) Durig, J. R.; Sullivan, J. F.; Geyer, T. J.; Godbey, S. E.; Little, T. S. *Pure Appl. Chem*. **1987**, *59*, 1327.
(21) Durig, J. R.; Shew, Z. *Vib. Spectrosc*. **1997**, *13*, 195.
(22) Rhee, K. H.; Snider. A. M.; Miller, F. A. *Spetrochim. Acta* **1973**, *A29*, 1029.
(23) Durig, J. R.; Brletic, P. A.; Li, Y. S.; Johnston, S. A.; Odom, J. D. *J. Chem. Phys*. **1981**, *75*, 1644.